

MEK1 and Protein Phosphatase 4 Coordinate *Dictyostelium* Development and Chemotaxis^{∇†}

Michelle C. Mendoza,^{1,2‡} Ezgi O. Booth,^{3,4‡} Gad Shaulsky,^{3,4} and Richard A. Firtel^{1*}

Section of Cell and Developmental Biology, Division of Biological Sciences, and Center for Molecular Genetics, University of California, San Diego, 9500 Gilman Drive, La Jolla, California 92093-0380¹; Biomedical Sciences Graduate Program, School of Medicine, University of California, San Diego, 9500 Gilman Drive, La Jolla, California 92093²; Graduate Program in Structural and Computational Biology and Molecular Biophysics, Baylor College of Medicine, Houston, Texas 77030³; and Department of Molecular and Human Genetics, Baylor College of Medicine, Houston, Texas 77030⁴

Received 22 November 2006/Returned for modification 22 January 2007/Accepted 6 March 2007

The MEK and extracellular signal-regulated kinase/mitogen-activated protein kinase proteins are established regulators of multicellular development and cell movement. By combining traditional genetic and biochemical assays with a statistical analysis of global gene expression profiles, we discerned a genetic interaction between *Dictyostelium discoideum mek1*, *smkA* (named for its role in the suppression of the *mek1*[−] mutation), and *pppC* (the protein phosphatase 4 catalytic subunit gene). We found that during development and chemotaxis, both *mek1* and *smkA* regulate *pppC* function. In other organisms, the protein phosphatase 4 catalytic subunit, PP4C, functions in a complex with the regulatory subunits PP4R2 and PP4R3 to control recovery from DNA damage. Here, we show that catalytically active PP4C is also required for development, chemotaxis, and the expression of numerous genes. The product of *smkA* (SMEK) functions as the *Dictyostelium* PP4R3 homolog and positively regulates a subset of PP4C's functions: PP4C-mediated developmental progression, chemotaxis, and the expression of genes specifically involved in cell stress responses and cell movement. We also demonstrate that SMEK does not control the absolute level of PP4C activity and suggest that SMEK regulates PP4C by controlling its localization to the nucleus. These data define a novel genetic pathway in which *mek1* functions upstream of *pppC-smkA* to control multicellular development and chemotaxis.

Multicellular morphogenesis requires the controlled movement of cell populations throughout a developing organism. Key to organized cell movement is chemotaxis, a highly regulated process of cell sensing, polarization, and movement up a chemical concentration gradient. *Dictyostelium discoideum* amoebae and human leukocytes utilize conserved signaling pathways and organelles for chemotaxis (1). *Dictyostelium* senses and moves by chemotaxis towards cyclic AMP (cAMP) during starvation and subsequent multicellular development (25, 34).

The MEK-extracellular signal-regulated kinase (ERK)/mitogen-activated protein kinase (MAPK) pathway is required for amoeboid chemotaxis and development in many systems (14, 27, 33, 35, 37, 48). MEKs are MAPK kinases that phosphorylate and activate ERKs/MAPKs, which then phosphorylate specific effector substrates (17, 31, 36). The conserved gene *smkA* (named for its role in the suppression of the *mek1*[−] mutation) is one of the few known regulators of the MEK pathway during amoeboid chemotaxis and development (30). The *Dictyostelium smkA* protein product (SMEK) functions in the nucleus during chemotaxis and is required for the manifestation of the *mek1*[−] mutant chemotaxis and developmental

defects (30). However, the genetic relationship between *mek1* and the second-site suppressor *smkA* is obscure due to the multifaceted chemotaxis and development phenotypes of the single and double *mek1*[−] and *smkA*[−] mutant strains (30).

In other systems, SMEK orthologs (named protein phosphatase 4 regulatory subunit 3 [PP4R3]) form a complex with the protein phosphatase 4 catalytic subunit (PP4C) and PP4R2 (12, 13, 15, 24). Protein phosphatase 4 (PP4) is a member of the PP2A subfamily of protein phosphatase P serine/threonine phosphatases (2). The PP4C-PP4R2-PP4R3 trimer has a conserved role in resistance to cisplatin and other cytotoxic agents (13, 45). *Saccharomyces cerevisiae* PP4C-PP4R2-PP4R3 specifically dephosphorylates γ H2AX during double-strand-break repair (24). *Caenorhabditis elegans* PP4R3 (SMK-1) controls the transcriptional response of DAF-16 to UV irradiation (24, 27, 44). PP4C and PP4R2 have also been implicated in the nucleation, stabilization, and growth of microtubules that connect chromatin to centrosomes (18, 39). The mechanism of PP4C regulation by PP4R2 and PP4R3 is unknown.

PP4C also independently forms complexes with the PP4R1 and α 4 regulatory subunits (12, 13). PP4C and PP4R1 form a binary complex (13, 16, 26) that inhibits the activity of histone deacetylase 3 (49). PP4C and α 4 interact with all eight subunits of an ATP-dependent chaperonin (the CCT complex) (12, 13).

Microarray profiles offer new hope for discerning unknown and complex genetic pathways due to their robust and quantitative nature. Investigators have used whole-genome expression phenotypes to accurately predict genetic interactions in the protein kinase A pathway without prior knowledge of the signaling network (41). We combined genetic and biochemical analyses with quantitative gene expression phenotype data in

* Corresponding author. Mailing address: Natural Sciences Building, Room 6316, University of California, San Diego, 9500 Gilman Dr., La Jolla, CA 92093-0380. Phone: (858) 534-2788. Fax: (858) 822-5900. E-mail: rafirtel@ucsd.edu.

† Supplemental material for this article may be found at <http://mcb.asm.org/>.

‡ These authors contributed equally.

∇ Published ahead of print on 12 March 2007.

order to elucidate the functional relationships among *mek1*, *smkA*, and *pppC* during development and chemotaxis.

We demonstrate that both *mek1* and *smkA* regulate the function of the *Dictyostelium* PP4C gene (*pppC*) during development and chemotaxis. We also show that catalytically active PP4C is required for *Dictyostelium* development and chemotaxis and the expression of many genes. SMEK positively regulates PP4C to induce a subset of PP4C's functions: developmental progression, chemotaxis, and the expression of genes specifically involved in cellular responses to stress and leading-edge formation during cell movement. *mek1* functions upstream of *pppC-smkA* to control chemotaxis in the opposite fashion. Interestingly, SMEK does not regulate PP4C by modulating the absolute level of PP4C activity. Rather, SMEK may regulate PP4C localization to the nucleus. We conclude that the complex *mek1-pppC-smkA* epistatic relationships define a novel genetic pathway critical for chemotaxis and multicellular development.

MATERIALS AND METHODS

Cloning of PP4C, PP4R1, and PP4R2. PP4C, PP4R1, and PP4R2 cDNA was obtained by reverse transcriptase PCR (RT-PCR) amplification from RNA made from *Dictyostelium* strain KAx-3 after 2 to 4 h of development with primers based on the predicted *pppC*, *ppr1*, and *ppr2* gene sequences in the *Dictyostelium* Genome Project database (<http://dictybase.org>; accession numbers DDB0185222, DDB0205616, and DDB0168233, respectively). In-frame mutagenesis by PCR was used to add an N-terminal FLAG epitope to PP4C, a V5 epitope to PP4R1, a T7 epitope to PP4R2, and a hemagglutinin (HA) epitope to SMEK and to obtain the H113Q mutant of PP4C (PP4C^{H113Q}). All expression constructs were cloned into the EXP-4(+) expression vector (11).

Knockout and overexpression cell lines. *Dictyostelium* KAx-3 cells were grown to log phase in axenic HL5 medium and transformed by electroporation (19). To knock out *pppC*, a blasticidin resistance gene cassette was inserted after the first 500 bp of the *pppC* coding sequence and the DNA was used to disrupt the resident allele by homologous recombination (40). For the overexpression of PP4C, PP4R1, PP4R2, and SMEK, cells were simultaneously electroporated with 20- μ g amounts of DNA for PP4C, PP4R1, and PP4R2 and with 40 μ g of DNA for SMEK. Transformants were selected in the presence of G418 (20 μ g/ml) and cloned by growth on nutrient agar plates in association with *Escherichia coli* strain B/r. Clones were screened by Western blotting to identify cells that simultaneously expressed the desired proteins. The *mek1*⁻ JH10 strain (37) was used to generate the *mek1*⁻ *pppC*⁻ double null strain.

Coimmunoprecipitation experiments. Cells (1×10^8 to 2×10^8) were harvested and lysed by resuspension in lysis buffer 1 (25 mM Tris-HCl [pH 6.8], 50 mM NaCl, 0.1% Nonidet P-40, 2 mM EDTA, 2 mM EGTA, 2 mM dithiothreitol, 1 mM ρ -amidinophenylmethanesulfonyl fluoride, 5 μ g/ml aprotinin, 5 μ g/ml leupeptin, 5 μ g/ml benzamide, 0.5 M NaF, 1 mM Na-PP_i, 1 mM vanadate). Lysates were cleared by centrifugation and incubated with anti-FLAG M2 gel (Sigma-Aldrich) or anti-HA affinity matrix (Roche) for 2 h at 4°C. Immunoprecipitates were washed four times with lysis buffer 1 containing 50 to 150 mM NaCl, and proteins were separated by sodium dodecyl sulfate-polyacrylamide gel electrophoresis. Semidry proteins were transferred onto nitrocellulose membrane (Millipore). Western blotting was performed using anti-HA.11 (Covance), anti-FLAG M2 (Sigma-Aldrich), and V5-10 anti-V5 (Sigma) antibodies at 1:1,000 dilutions in 5% nonfat dry milk.

Development and chemotaxis analysis. Developmental morphology was observed by plating washed log-phase cells onto nonnutrient 12 mM Na⁺ and K⁺ (Na⁺-K⁺) phosphate buffer agar plates and photographing at the times indicated in the figures.

For chemotaxis analysis, cells were exposed to pulses of 30 nM cAMP in Na⁺-K⁺ phosphate buffer every 6 min for 5 h (29). The cells were then deposited on glass-bottomed microwell plates. A micropipette containing 150 μ M cAMP was positioned near the cells by using a micromanipulator (Eppendorf-Netheler-Hinz GmbH), and chemotaxis was recorded by acquiring differential interference contrast images every 6 s. Cell polarity and directionality and the speed of centroid movement were calculated for populations of cells moving by chemotaxis by using the DIAS image analysis computer software (43).

PP4 Ser/Thr phosphatase assays. Cells were pulsed with cAMP as mentioned above and lysed in lysis buffer 2 (lysis buffer 1 without NaF, Na-PP_i, or vanadate). For the *p*-nitrophenyl phosphate (pNPP) phosphatase assay, lysates were incubated with anti-FLAG M2 gel (Sigma-Aldrich) for 2 h at 4°C. The PP4C immunoprecipitates were collected by centrifugation and washed three times with buffer containing 25 mM Tris-HCl (pH 6.8), 200 mM NaCl, 0.1% Nonidet P-40, 2 mM EDTA, 2 mM EGTA, 2 mM dithiothreitol, and protease inhibitors. The immunoprecipitated protein beads were then washed once with assay buffer (50 mM Tris-HCl, pH 7.0, and 0.1 mM CaCl₂) and preincubated with assay buffer containing 0.1 mg/ml bovine serum albumin (BSA) and 1 mM MnCl₂ at 37°C for 15 min. The reactions were initiated by adding 0.9 mg/ml pNPP (dissolved in 50 mM Tris-HCl, pH 7.0), carried out at 37°C for 30 min, and then stopped with 1.3% K₂HPO₄, and results were read at 405 nm.

For the malachite green phosphatase assays, lysates were incubated with anti-T7 agarose (Novagen) for 2 h at 4°C with 2 mg of BSA to immunoprecipitate T7-PP4R2. Immunoprecipitates were collected by centrifugation and washed three times with lysis buffer 2 containing 100 mM NaCl and once with assay buffer (50 mM Tris-HCl, pH 7.0, and 0.1 mM CaCl₂). Immunoprecipitates were incubated with 50 μ M KRpTIRR peptide from the Ser/Thr phosphatase assay kit 1 (Upstate Biotechnology) in 40 μ l of assay buffer containing 0.1 mg/ml BSA and 1 mM MnCl₂ at 30°C. Peptide in buffer was used as a negative control. The assay was terminated by pelleting the immunoprecipitates; transferring the assay buffer to a 96-well, half-volume plate; and adding 100 μ l of malachite green solution over 10 min at room temperature. The assay results were read at 630 nm with an MRX Revelation microplate reader (Dynex Technologies).

Microarray experiments. Cells were developed on 2% agar plates made with 12 mM Na-K phosphate buffer, pH 6.4. Cells were collected after 0, 6, 12, and 18 h of development and resuspended in TRIzol reagent (Life Technologies), and RNA was extracted according to the manufacturer's recommended protocol. Each strain was developed three times independently (biological replication), and each RNA sample was analyzed twice on separate microarrays (technical replication). The microarrays included nearly 5,000 nonredundant targets, each printed in duplicate on the arrays. The microarrays contained most of the nonredundant cDNA clones identified by the Japanese *Dictyostelium* cDNA project (42), so they represented most of the vegetatively and developmentally expressed genes in the *Dictyostelium* genome. The above-mentioned procedures and the microarray data normalization were carried out as described previously (41).

ANOVA. Differentially expressed genes were identified by the analysis of variance (ANOVA) of microarray data from five mutants and one wild-type strain. First, we concatenated all of the replications of all of the time course data from all of the mutants into one matrix. We then used the "aov()" function in the R statistical software to identify genes with *P* values of <0.05. The determining factor was the genotype, while time and replication (both biological and technical) were considered as well. This procedure ensured that we identified genes whose temporal patterns of expression varied due to genotype rather than technical error.

Epistasis analysis. The epistatic relationships between mutated genes were determined by comparing the distances between the quantitative phenotypes of two mutants with individual mutations and that of the respective double mutant as described previously (43, 50). For the transcriptional profiles, replicate data on each gene were averaged for each mutant and concatenated into one vector (the dimensionality of the vector equals the number of genes on the microarray times the number of time points, about 20,000). Euclidian distances between the vectors were calculated using the "dist()" function in R. Three types of data were used to calculate distances: (i) all of the genes present on the microarray, (ii) genes differentially expressed according to the ANOVA, and (iii) chemotaxis and enzyme activity measurements for the mutants (PP4C activity and cell speed, directionality, and roundness). Data of types i and ii were essentially identical (data not shown), so only type i data are shown. Each class of measurements was normalized to 1 by dividing the data by the highest value in the class.

To visualize the dissimilarity between the strains, we conducted hierarchical clustering of the strains based on the calculated distances by using the "pvlust()" function in R and displayed the data as dendrograms. The same function was used to calculate the *P* values by multiscale bootstrap resampling. Specific Euclidian distances between the mutants, normalized to 1 as described previously (41), are also shown as sides of triangles.

RESULTS

Classical genetics reveal a complex *mek1-pppC-smkA* interaction during multicellular development and chemotaxis. We

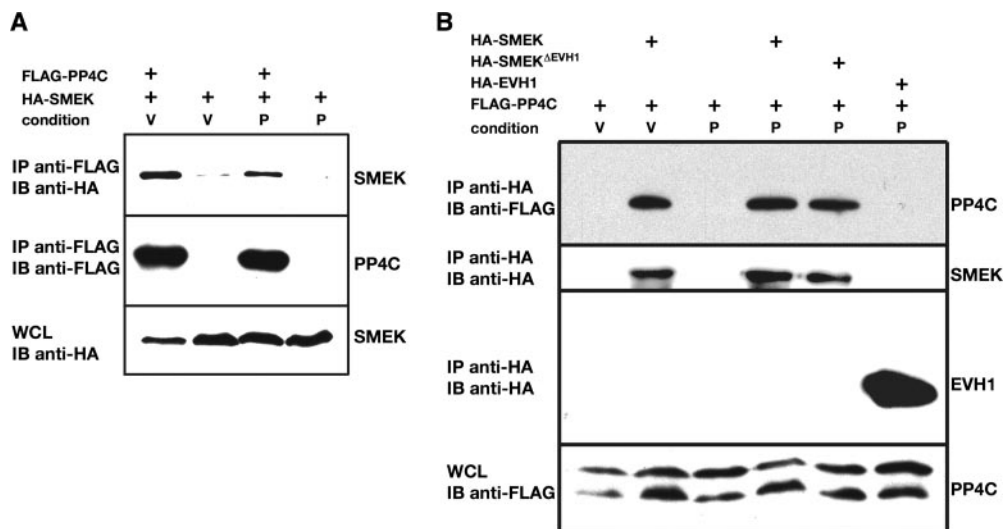


FIG. 1. Protein-protein interactions in the PP4 complex. Cells expressing various combinations of FLAG-PP4C, HA-SMEK, HA-SMEK^{ΔEVH1}, and/or HA-EVH1 as indicated (+, present) were lysed, and the proteins were immunoprecipitated with anti-FLAG (A) or anti-HA (B) antibodies. The immunoprecipitates were analyzed by Western blotting with the indicated antibodies. V, vegetative cells; P, cells pulsed with 30 nM cAMP for 5 h; IP, immunoprecipitation; IB, immunoblotting; WCL, whole-cell lysate.

set out to discern the epistatic relationships between *mek1*, the *smkA* gene associated with the suppression of the *mek1*⁻ mutation, and the gene encoding the putative SMEK interactor, *pppC*. The *Dictyostelium* genome contains one copy of the *pppC* gene (accession number DDB0185222), which is predicted to encode the catalytic subunit of PP4. *Dictyostelium* also contains *pprA* and *pprB* (accession numbers DDB0205616 and DDB0168233), which are predicted to encode PP4R1 and PP4R2, respectively. We cloned the respective cDNA sequences by RT-PCR from mRNA collected from cells at 2 to 4 h of development.

We first determined if, like their orthologs in other systems, *Dictyostelium* PP4C and SMEK physically interact. We epitope tagged and expressed the respective proteins (FLAG-PP4C and HA-SMEK) in wild-type *Dictyostelium* KAx-3 cells. We extracted the proteins from vegetative cells and from developing cells that were brought to chemotactic competence by cAMP pulsing (20). The proteins were immunoprecipitated with antibodies against the tags and resolved by sodium dodecyl sulfate-polyacrylamide gel electrophoresis. Protein-protein interactions were detected by Western blotting with antibodies against the other subunits. HA-SMEK coimmunoprecipitated with FLAG-PP4C, and the interaction was not developmentally regulated (Fig. 1A). A reciprocal anti-HA immunoprecipitation step confirmed that the *pppC* gene product physically interacts with SMEK during *Dictyostelium* growth and multicellular development (Fig. 1B). SMEK's EVH1 domain constitutively localizes to the cell cortex, while a SMEK mutant lacking the EVH1 domain (SMEK^{ΔEVH1}) constitutively localizes to the nucleus (30). We examined the SMEK mutants for their ability to coimmunoprecipitate with PP4C and found that HA-SMEK^{ΔEVH1} physically interacts with FLAG-PP4C but HA-EVH1 does not. Thus, FLAG-PP4C does not nonspecifically coimmunoprecipitate with all overexpressed HA-SMEK proteins (Fig. 1B). We noted that FLAG-PP4C appeared as a doublet in some of our whole-cell lysate Western blots. We

have not further characterized the two FLAG-PP4C species, but they may be the result of protein modification and/or degradation. Attempts to coimmunoprecipitate the PP4C-PP4R2-SMEK heterotrimeric complex were unsuccessful due to the toxicity of simultaneously overexpressing all three members of the complex. We previously observed an inhibition of cell growth with the overexpression of SMEK itself (30).

We next generated *pppC*⁻ and *mek1*⁻ *pppC*⁻ double null strains via homologous recombination of the *pppC* gene in wild-type and *mek1*⁻ cells (data not shown). Upon starvation, *Dictyostelium* cells secrete oscillatory waves of the chemoattractant cAMP, which induce the expression of signaling proteins involved in sensing and chemotactically responding to extracellular cAMP. Wild-type *Dictyostelium* cells form aggregates of ~10⁵ cells (9 h), differentiate, and chemotactically sort into groups of specific cell types. The organism then extends a tip from the mound (12 h), transforms into a migrating slug (16 h), and differentiates into a fruiting body with a stalk and a sorus containing spores (24 h) (3, 10, 28). *mek1*⁻ cells form tiny mounds, and their multicellular morphogenesis is accelerated relative to that of wild-type cells (27, 30). We noticed that following aggregation (Fig. 2A), *pppC*⁻ cells exhibited attenuated development. The majority (approximately two-thirds) of the aggregates permanently remained as mounds while approximately one-third belatedly transitioned into slugs and stunted stalks and fruiting bodies after 24 to 36 h of starvation (Fig. 2A; data not shown). The delay of *pppC*⁻ cells in exiting from the mound stage was remarkably similar to, but more severe than, that of *smkA*⁻ cells (Fig. 2A). We also found that the inactivation of PP4C in *mek1*⁻ cells (*mek1*⁻ *pppC*⁻ strain) partially suppressed the tiny, precocious mound development phenotype of the *mek1*⁻ strain. This suppression was similar to the effects of inactivating SMEK in *mek1*⁻ cells (Fig. 2A). The similarity between the *smkA*⁻ and *pppC*⁻ developmental phenotypes suggests that *smkA* and *pppC* participate in one pathway. The increased severity of the mound arrest phenotype

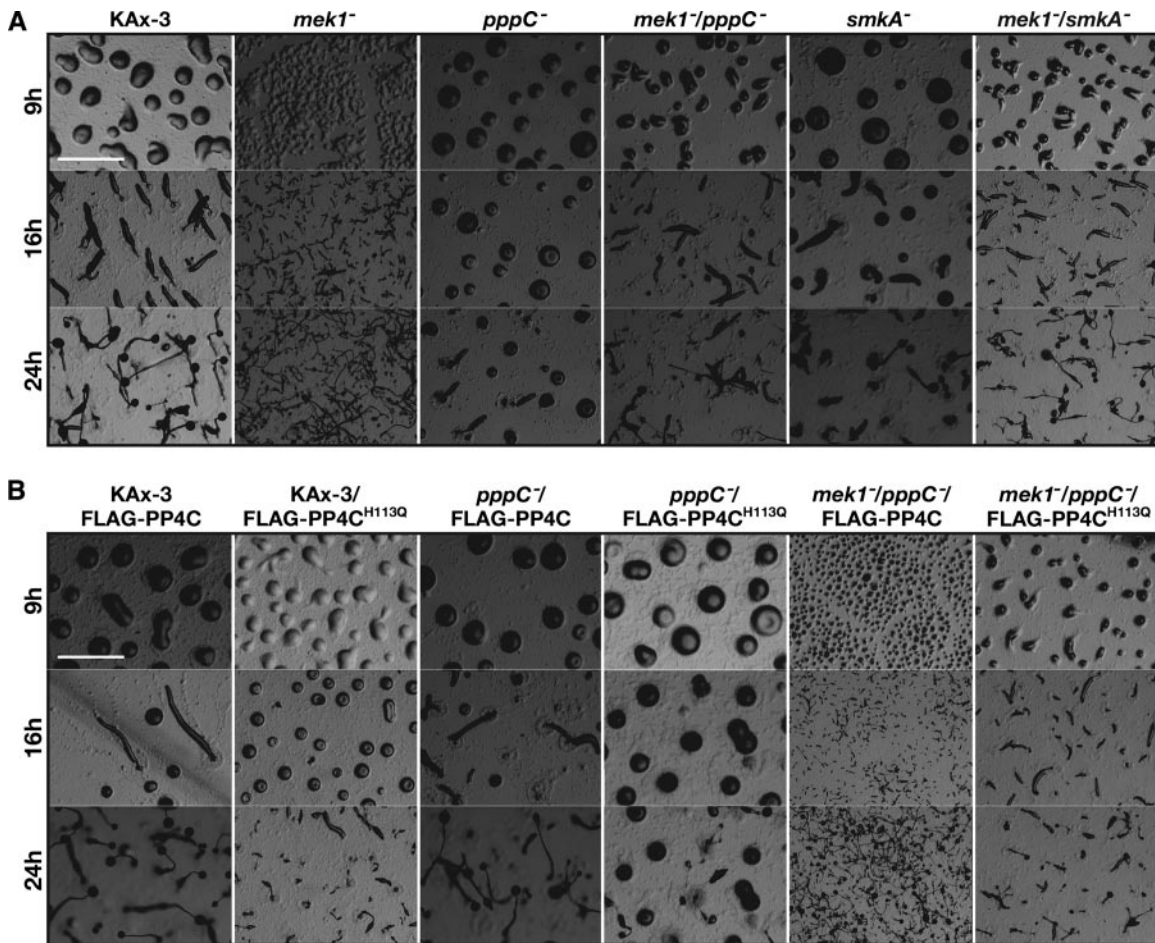


FIG. 2. The PP4 complex affects developmental morphology. Cells were developed on 12 mM Na⁺-K⁺ phosphate agar plates for the indicated times, and photographs were taken (bars = 1 mm). Developing wild-type cells form aggregates (9 h), protrude a mound tip (12 h), transform into a migrating slug (16 h), and differentiate into stalks and fruiting bodies (24 h).

among *pppC*⁻ cells, compared to that among *smkA*⁻ cells, indicates that during development, *pppC* also has some functions independent of *smkA*. The suppression of the *mek1*⁻ tiny, precocious mound development phenotype by the *smkA*⁻ and *pppC*⁻ mutations suggests that *smkA* and *pppC* function together, downstream of *mek1*. However, the loss of MEK1 partially alleviates the developmental delay in *pppC*⁻ and *smkA*⁻ cells, which is inconsistent with a linear *mek1*-*pppC*-*smkA* pathway. Possible explanations for the conflicting data include the idea that *mek1* and *pppC*-*smkA* function in parallel pathways and/or that *pppC*-*smkA* feeds back to modulate *mek1*'s functional output.

The loss of *smkA* also suppresses the *mek1*⁻ mutant cell polarity and chemotaxis defects (27, 30, 37). Thus, we tested whether PP4C activity is required for the manifestation of the *mek1*⁻ chemotaxis phenotype. We examined the responses of *pppC*⁻ and *mek1*⁻ *pppC*⁻ double null cells to a gradient of the chemoattractant cAMP. Wild-type KAx-3 cells move by chemotaxis at a speed of ~10 μm/min, with 50% roundness and a directionality of 0.71 (indicating polarization and movement up the chemoattractant gradient with few turns) (Fig. 3; Table 1). In contrast, *mek1*⁻ cells move with significantly reduced speed, polarization, and directionality (30, 37). The

loss of PP4C in an otherwise wild-type background (*pppC*⁻) had negligible effects on chemotaxis speed, cell polarization, or the frequency of direction change. However, the loss of PP4C in *mek1*⁻ cells suppressed the *mek1*⁻ mutant chemotaxis defects. *mek1*⁻ *pppC*⁻ double null cells moved at a speed of ~9 μm/min with 47% roundness and a directionality of 0.73 (Fig. 3; Table 1). Therefore, like SMEK, PP4C is required for the manifestation of the *mek1*⁻ mutant cell polarization and chemotaxis defects. The similarity between the *smkA*⁻ and *pppC*⁻ chemotaxis phenotypes suggests that the two genes participate in one pathway. Interestingly, in the case of chemotaxis, the *pppC*⁻ and *smkA*⁻ mutant phenotypes exhibit nearly identical levels of severity, suggesting that all of the chemotaxis functions of *pppC* involve *smkA*.

The phosphatase activity of PP4C is essential for its function during development and chemotaxis. To be sure that the observed *pppC*⁻ development and chemotaxis phenotypes were due to a lack of PP4C activity, we eliminated PP4C activity by site-directed mutagenesis and tested whether the mutated allele could complement the *pppC*⁻ phenotype. Histidine 113 in *Dictyostelium* PP4C is an invariable and essential amino acid found in all protein phosphatase P family members. It is predicted to function as a general acid that protonates the

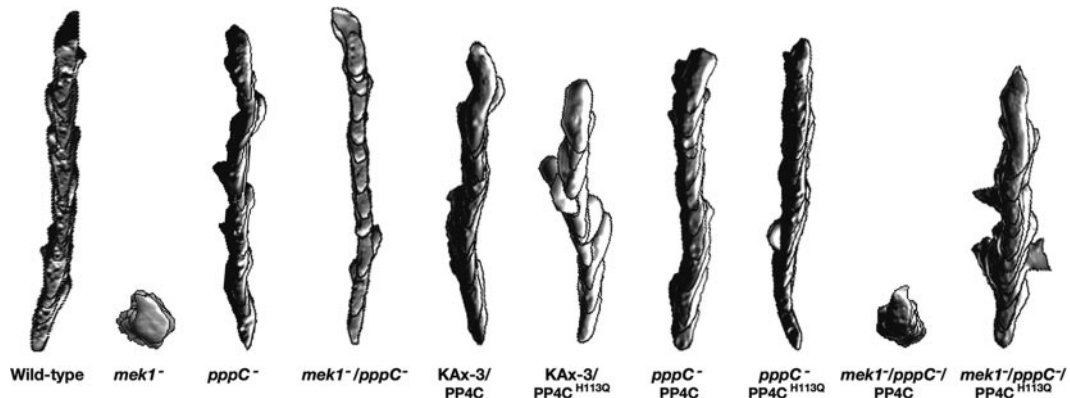


FIG. 3. The PP4 complex regulates chemotaxis. Images show representative tracings of cells moving towards a micropipette filled with 150 μM cAMP. Time lapse recordings were taken at 6-s intervals; superimposed images show the cell shapes and directions and the length of the path at 1-min intervals for 11 min.

leaving-group oxygen and accelerates dephosphorylation (4, 5, 32). We expressed FLAG-PP4C and FLAG-PP4C^{H113Q} in wild-type *Dictyostelium* cells, immunoprecipitated the PP4 complex with anti-FLAG antibodies, and performed a phosphatase assay using pNPP as a substrate. As expected, the phosphatase activity of the mutated protein (FLAG-PP4C^{H113Q}) towards pNPP was indistinguishable from the background activity (data not shown). When overexpressed in wild-type cells, FLAG-PP4C^{H113Q} replicated the delay of *pppC*⁻ mutants in exiting from the mound stage, whereas FLAG-PP4C overexpression had no obvious phenotype (Fig. 2B). This finding suggests that the H113Q mutant functions in a dominant negative manner, possibly by sequestering endogenous PP4C regulatory subunits or substrates. FLAG-PP4C complemented the *pppC*⁻ mound arrest phenotype and abolished the suppression of the *mek1*⁻ mutant defects, while FLAG-PP4C^{H113Q} did not (Fig. 2B). FLAG-PP4C also complemented the *pppC*⁻ mutant chemotaxis defects in *mek1*⁻ *pppC*⁻ double null cells, whereas FLAG-PP4C^{H113Q} did not.

mek1⁻ *pppC*⁻ double null FLAG-PP4C-expressing cells polarized and were poorly chemotactic, like *mek1*⁻ cells (3 $\mu\text{m}/\text{min}$ at 79% roundness, with a directionality of 0.19), but *mek1*⁻ *pppC*⁻ double null FLAG-PP4C^{H113Q} cells were chemotactically like *mek1*⁻ *pppC*⁻ double null cells and wild-type cells (7 $\mu\text{m}/\text{min}$ at 54% roundness, with a directionality of 0.65) (Fig. 3; Table 1). We conclude that PP4C activity is required for a timely exit from the mound stage and the manifestation of the *mek1*⁻ mutant defects in development, chemotaxis speed, and cell polarization and directionality.

Quantitative epistasis analysis determines that *smkA* and *pppC* function downstream of *mek1*. PP4C has biological functions in addition to its role in controlling development and chemotaxis, which may or may not involve *mek1* and *smkA* (9, 24). These and several of our own findings precluded a clear delineation of the intergene relationships by using traditional types of analysis. To better understand the *mek1*, *smkA*, and *pppC* genetic interactions, we utilized epistasis analysis of quantitative phenotypes. Epistasis analysis can be performed

TABLE 1. Chemotaxis and phosphatase activity parameters^a

Strain name or description	Speed ($\mu\text{m}/\text{min}$) ^b	Directionality ^c	Roundness (%) ^d	Phosphatase ^e activity (pmol)
KAx-3	9.9 \pm 1.4	0.71 \pm 0.08	50 \pm 3	221 \pm 19
<i>mek1</i> ⁻	3.5 \pm 0.3	0.13 \pm 0.04	74 \pm 4	179 \pm 18
<i>pppC</i> ⁻	9.7 \pm 1.0	0.67 \pm 0.04	56 \pm 2	71 \pm 10
<i>mek1</i> ⁻ <i>pppC</i> ⁻	9.3 \pm 1.1	0.73 \pm 0.05	47 \pm 2	60 \pm 15
<i>smkA</i> ⁻	8.6 \pm 0.4	0.76 \pm 0.05	47 \pm 2	219 \pm 31
<i>mek1</i> ⁻ <i>smkA</i> ⁻	10.0 \pm 1.3	0.67 \pm 0.04	48 \pm 2	195 \pm 16
KAx-3 strain expressing FLAG-PP4C	8.2 \pm 1.0	0.78 \pm 0.02	57 \pm 2	ND
KAx-3 strain expressing FLAG-PP4C ^{H113Q}	8.5 \pm 1.7	0.45 \pm 0.06	61 \pm 2	ND
<i>pppC</i> ⁻ strain expressing FLAG-PP4C	10.0 \pm 1.2	0.75 \pm 0.07	63 \pm 1	ND
<i>pppC</i> ⁻ strain expressing FLAG-PP4C ^{H113Q}	10.3 \pm 1.0	0.77 \pm 0.06	59 \pm 5	ND
<i>mek1</i> ⁻ <i>pppC</i> ⁻ strain expressing FLAG-PP4C	2.9 \pm 0.7	0.19 \pm 0.07	79 \pm 5	ND
<i>mek1</i> ⁻ <i>pppC</i> ⁻ strain expressing FLAG-PP4C ^{H113Q}	7.3 \pm 0.7	0.65 \pm 0.04	54 \pm 1	ND

^a Chemotaxis towards a micropipette filled with 150 μM cAMP was monitored by time lapse recordings as shown in Fig. 3, and the cells' parameters of movement were calculated using DIAS software. Numbers are means \pm the standard errors of the means of results for at least five cells (110 frames/cell).

^b Speed of the cells' centroid movement along the total path length.

^c Directionality is a measurement of the linearity of the path. Cells moving in a straight line to the needle have a directionality of 1.00.

^d Roundness is a measurement of the lack of cell polarity. A high percentage of roundness indicates that the cells are rounder and less polarized.

^e Phosphatase activity in T7-PP4R2 immunoprecipitates (picomoles of phosphate released from a phosphopeptide substrate) was determined as described in the legend to Fig. 6B by using conditions under which the assay was linear: lysate from $\times 10^8$ cells and a 25-min assay duration. Numbers are means \pm the standard errors of the means of results from at least three replicate phosphatase assays. ND, not determined.

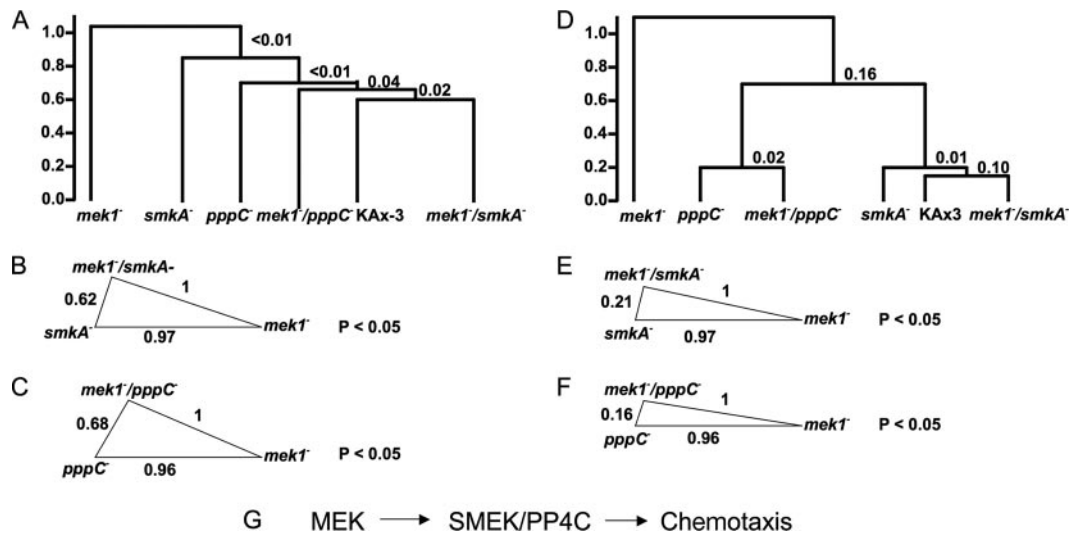


FIG. 4. Quantitative epistasis analysis. Quantitative gene expression and chemotaxis phenotypes of *smkA*⁻, *pppC*⁻, *mek1*⁻, *mek1*⁻ *smkA*⁻ double null, *mek1*⁻ *pppC*⁻ double null, and wild-type (KAx-3) cells during development were analyzed. (A) Hierarchical clustering dendrogram based on the differences (Euclidian distances) between the mutants' microarray phenotypes. Each value at the branch splitting points is the *P* value calculated by multiscale bootstrap resampling. (B) Euclidian distances between microarray phenotypes of *smkA*⁻, *mek1*⁻, and *mek1*⁻ *smkA*⁻ double null cells were calculated and are presented as the edges of a triangle. Numbers indicate lengths (distances). *P* values for distances were calculated by random sampling ($n = 1,000$). (C) Euclidian distances between microarray phenotypes of *pppC*⁻, *mek1*⁻, and *mek1*⁻ *pppC*⁻ double null cells were calculated and are presented as the edges of a triangle. Numbers indicate lengths (distances). *P* values for distances were calculated by random sampling ($n = 1,000$). (D) Hierarchical clustering dendrogram based on the differences (Euclidian distances) between the mutants' chemotaxis phenotypes (cell speed, directionality, and roundness and PP4C activity during chemotaxis). Values at the branch splitting points are the *P* values calculated by multiscale bootstrap resampling. (E) Euclidian distances between the morphology phenotypes of *smkA*⁻, *mek1*⁻, and *mek1*⁻ *smkA*⁻ double null cells were calculated and are presented as described in the legend to panel B. (F) Euclidian distances between morphology phenotypes of *pppC*⁻, *mek1*⁻, and *mek1*⁻ *pppC*⁻ double null cells were calculated and are presented as described in the legend to panel B. (G) A genetic pathway was inferred from the epistatic relationships.

on two strains (for example, x and y) carrying mutations in two different genes, if the strains exhibit different phenotypes (X and Y). If a third strain carrying both mutations (xy) exhibits a phenotype identical to that of one of the original strains (Y), then that phenotype is epistatic to the other (Y is epistatic to X). In a signaling pathway, the epistatic gene is thought to function downstream of the other gene (50). We have previously shown that when analyzing quantitative phenotypes, the degree of similarity between the mutants can be determined by comparing the difference (or statistical Euclidian distance) between the values of their respective phenotypes (22, 41). This statistical approach has been very powerful in elucidating genetic relationships involving complex data sets. We first performed microarray phenotyping, in which global expression profiles of strains include quantitative, unbiased phenotypes not specific to any particular biological process (41).

Six strains (*mek1*⁻, *pppC*⁻, *smkA*⁻, *mek1*⁻ *pppC*⁻ double null, and *mek1*⁻ *smkA*⁻ double null strains and the parental wild-type strain KAx-3) were starved and developed on phosphate-buffered agar. RNA was collected from cells after 0, 6, 12, and 18 h and analyzed with a microarray including most of the genes expressed in *Dictyostelium* (41). (All of the microarray data are provided in a supplement according to the minimum information about a microarray experiment format and can be found at http://dictygenome.org/supplement/gadi/mendoza_2006.) To determine the degrees of similarity between the strains, we computed the differences (Euclidean distances) between the strains based on measurements at four time points

for 5,624 array targets. We then used hierarchical clustering to generate a dendrogram (Fig. 4A) that summarizes the quantitative distances between the six strains. In this representation, two strains that are more similar to each other than either is to a third strain are directly connected on the tree structure. The vertical lengths of the branches are directly proportional to the differences between the strains. The statistical significance of the dendrogram relationships was calculated by multiscale bootstrap resampling (41), and the results were highly significant in all cases.

The wild-type and *mek1*⁻ *smkA*⁻ double null strains clustered on the same branch in the microarray phenotype dendrogram, indicating that their gene expression profiles are the most similar. The *mek1*⁻ strain is the most dissimilar strain, as it clustered away from all of the other strains on a separate branch (Fig. 4A). The dendrogram and individual distance calculations indicate that the *mek1*⁻ *smkA*⁻ double mutant is more similar to the *smkA*⁻ single mutant than to the *mek1*⁻ single mutant (Fig. 4A and B). Additionally, the *mek1*⁻ *pppC*⁻ double mutant is more similar to the *pppC*⁻ single mutant than to the *mek1*⁻ single mutant (Fig. 4A and C). We used these measurements to perform genetic epistasis analysis. Because the *mek1*⁻ *smkA*⁻ and *mek1*⁻ *pppC*⁻ double mutants are more similar to *smkA*⁻ and *pppC*⁻ mutants than to *mek1*⁻ cells, *smkA* and *pppC* are epistatic to *mek1* (Fig. 4G).

To compare the unbiased intergene relationship of *mek1*, *smkA*, and *pppC* to their specific relationship during chemotaxis, we calculated the differences (Euclidian distances) between the six strains by using the available phenotypic assays

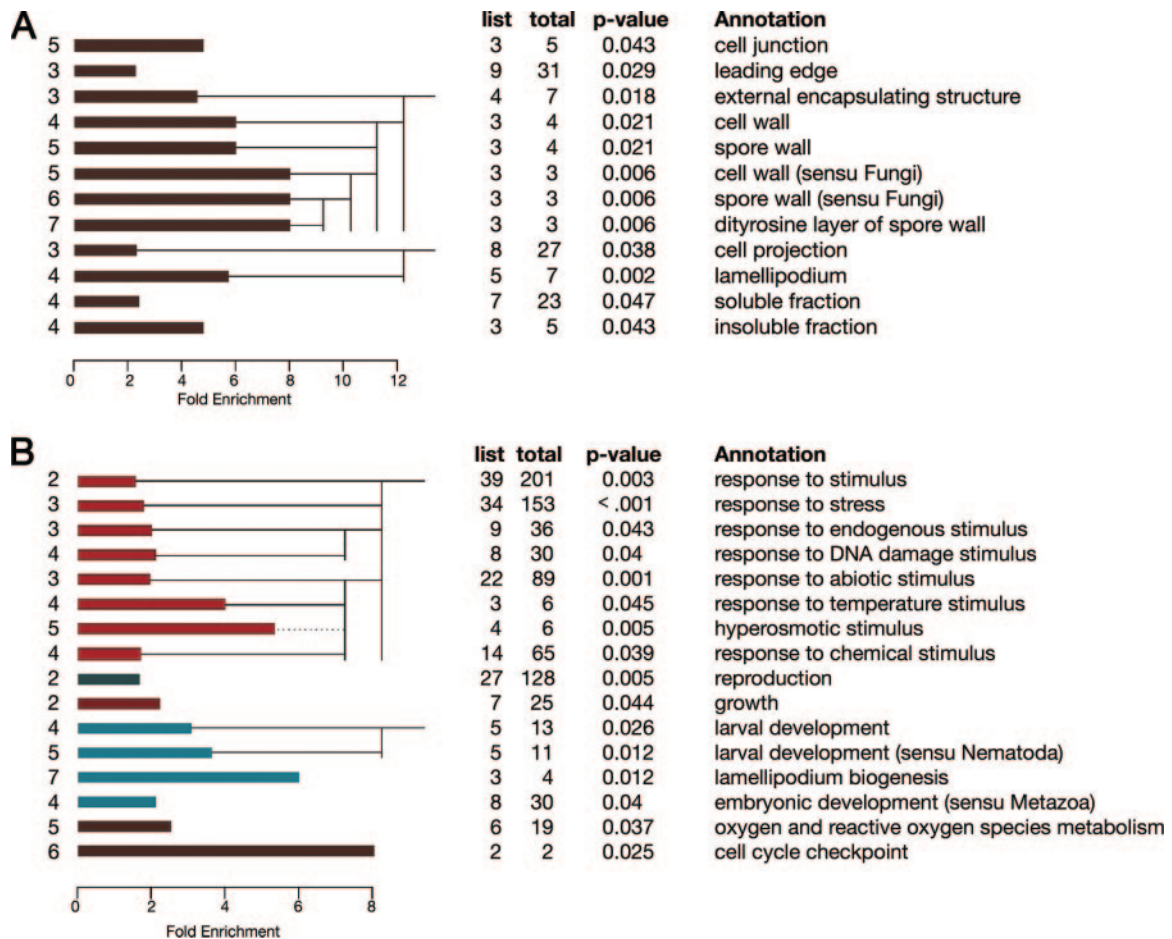


FIG. 5. Gene ontology analysis of 498 differentially expressed genes. We examined the 498 genes differentially expressed among the six mutants for gene ontology annotation enrichment. Bar lengths indicate the levels of enrichment (*n*-fold) for gene ontology terms (scales below graphs), and the gene ontology levels are indicated by the numbers to the left. The branching patterns indicate derivative annotations (e.g., the dityrosine layer of the spore wall is a specific case of spore wall [sensu Fungi]). The numbers under the heading “list” indicate the numbers of genes in the list of 498 genes with the respective annotations, the numbers under the heading “total” indicate the total numbers of genes found on the entire microarray with the respective annotations, and *P* values indicate the statistical significance of the enrichment. Enrichments for gene ontology annotations indicating cellular components (A) and biological processes (B) are shown. Annotations such as “embryonic development” are derived from sequence homology analysis and indicate that the *Dictyostelium* genes are homologous to genes in other organisms that have the indicated annotations.

with measurable results: PP4 activity in developing, chemotaxis-competent cells and chemotaxis cell speed, directionality, and roundness (Table 1). The presence of endogenous phosphatase activity associating with PP4R2 immunoprecipitates in six strains, the wild-type KAx-3, *mek1*⁻, *pppC*⁻, *smkA*⁻, *mek1*⁻ *pppC*⁻ double null, and *mek1*⁻ *smkA*⁻ double null strains, was assayed (Table 1). As expected, the phosphatase activity in *pppC*⁻ and *mek1*⁻ *pppC*⁻ double null cells was reduced (to about one-third) compared to the activity in the corresponding KAx-3 and *mek1*⁻ cells, indicating that the immunoprecipitated activity was PP4C specific. The differences between the phosphatase activity and chemotaxis measurements were summarized (see Materials and Methods) and analyzed by hierarchical clustering to generate a dendrogram (Fig. 4D). The statistical significance of the findings in the dendrogram was calculated by multiscale bootstrap resampling (41), and the findings were highly significant in all cases. It should be noted that for the epistasis analysis, the phenotypes described in

Table 1 were considered to be independent of one another and to have equal weights. The numerical values were normalized to ensure equal weights.

In the analysis specific to chemotaxis, the wild-type KAx-3 and *mek1*⁻ *smkA*⁻ double null strains clustered on the same branch with *smkA*⁻ cells, indicating that their chemotaxis and phosphatase activity phenotypes are the most similar (Fig. 4D). The *pppC*⁻ and the *mek1*⁻ *pppC*⁻ double null strains clustered together on a separate branch that joins the branch with the wild-type, *mek1*⁻ *smkA*⁻ double null, and *smkA*⁻ strains. Most importantly, both *mek1*⁻ *smkA*⁻ and *mek1*⁻ *pppC*⁻ double mutants clustered on the same main branch as the respective *smkA*⁻ and *pppC*⁻ single mutants, while the single *mek1*⁻ mutant formed an out-group. This separation of the *pppC*⁻ strain and *smkA*⁻ strain branches is inconsistent with the microarray phenotype dendrogram and may be due to the influence of SMEK-independent PP4C activity in the phosphatase assays. However, the clustering of the *mek1*⁻ mutant on a

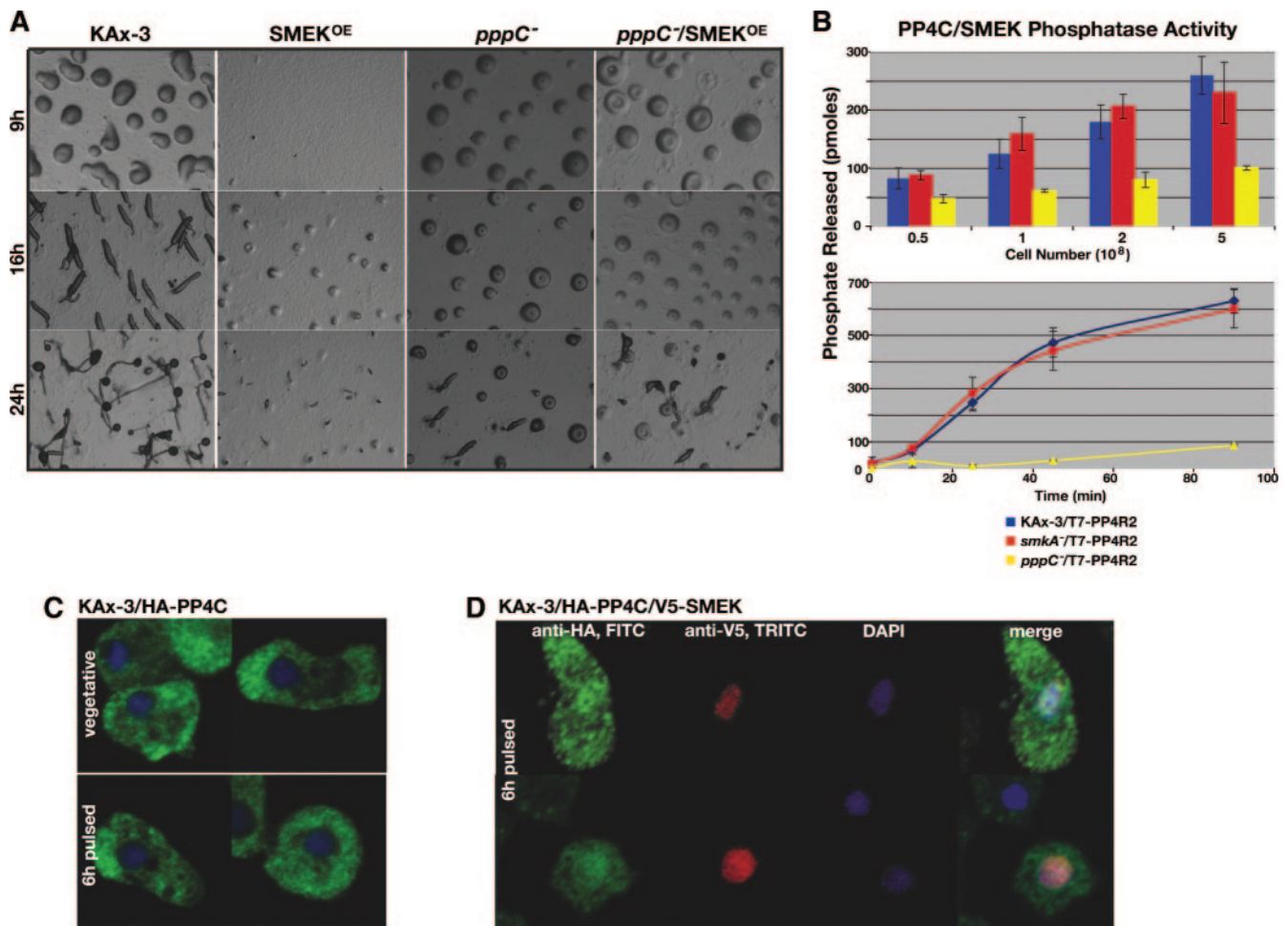


FIG. 6. SMEK regulates PP4C subcellular localization, and PP4C is epistatic to SMEK. (A) Cells were developed on 12 mM Na⁺-K⁺ phosphate agar plates for the indicated times, and photographs were taken. Multicellular developmental morphology at 9 h (wild-type mound stage), 16 h (wild-type slug stage), and 24 h (wild-type stalk and fruiting body stage) is depicted. SMEK^{OE}, cells overexpressing SMEK; pppC⁻/SMEK^{OE}, pppC⁻ cells overexpressing SMEK. (B) Serine/threonine phosphatase activity in T7-PP4R2 immunoprecipitates as a function of the protein input (number of cells lysed and used in immunoprecipitation) and the length of time of the assay. (C) HA-PP4C localization in vegetative KAx-3 HA-PP4C-expressing cells and in KAx-3 HA-PP4C-expressing cells moving by chemotaxis. (D) HA-PP4C and V5-SMEK localization in KAx-3 HA-PP4C- and V5-SMEK-expressing cells moving by chemotaxis. FITC, fluorescein isothiocyanate; TRITC, tetramethyl rhodamine isocyanate; DAPI, 4',6'-diamidino-2-phenylindole.

separate branch is consistent with the microarray-based observation that the *mek1*⁻ chemotaxis phenotype is quantitatively the most different of all those of the six strains. The individual distance calculations indicate that the *mek1*⁻ *smkA*⁻ double mutant is more similar to the *smkA*⁻ single mutant than to the *mek1*⁻ single mutant (Fig. 4E). The *mek1*⁻ *pppC*⁻ double mutant is more similar to the *pppC*⁻ single mutant than to the *mek1*⁻ single mutant (Fig. 4F). These results confirm our phenotypic conclusions that during developmentally induced chemotaxis, *smkA* and *pppC* function epistatically to (or downstream of) *mek1* in a linear pathway (Fig. 4G).

The *mek1*-*pppC*-*smkA* pathway regulates gene expression for cell motility and stress response. To further characterize the *mek1*⁻, *smkA*⁻, and *pppC*⁻ mutant gene expression phenotypes, we examined which groups of coregulated genes were differentially regulated in the mutants. By analyzing coexpressed gene families, rather than individual genes, we avoided problems with microarray noise (23, 46, 47). Variations in gene

expression patterns among strains in our experiments could stem from the genotypes, developmental times, and experimental variation. To identify differentially regulated genes, we concatenated all of the microarray data from all of the mutants and used ANOVA to identify genes for which differential expression was attributable to genotype effects ($P < 0.05$) but not to experimental variation. Based on these criteria, we identified 498 genes that were differentially expressed among the six mutants (see Table S1 in the supplemental material). We verified the microarray results by testing the expression of five of the genes (*crIA*, *racE*, *limB*, *wimA*, and *proA*) in all six strains by real-time RT-PCR. We found that 26 of the 30 comparisons exhibited a positive correlation between the microarray and real time RT-PCR data, validating the microarray results (see Fig. S1 in the supplemental material). We then tested whether these genes participate in known functions by using the gene ontology analysis tool GOAT (47). An examination of the predicted subcellular localization of the gene products indi-

cated that they likely function in the leading edge, cell projection, and/or lamellipodium (Fig. 5A). These compartments participate in cell motility, in agreement with our finding that the PP4 pathway regulates chemotaxis in *Dictyostelium*. An examination of the biological processes prevalent in association with the PP4-regulated genes revealed a large number of stimulus and stress response genes, including those involved in the response to DNA damage (Fig. 5B). The role of human and yeast PP4C in inducing a transcriptional response to DNA damage is well established (9, 24).

Gene expression analyses of a variety of wild-type and mutant *Dictyostelium* strains have revealed 16 gene expression modes (or categories) in which coexpression is highly associated with common functions (6). We tested the distribution of these modes among 498 PP4-regulated genes and found significant overrepresentation of four modes (see Table S2 in the supplemental material). Of particular interest were modes 9 and 15, which were overrepresented among genes encoding calcium binding proteins, and mode 13, which was overrepresented among genes encoding drug transport proteins and proteins involved in DNA damage response. Mode 15 is also highly represented among chemotaxis genes (6). These findings correlate the *mek1-pppC-smkA* pathway with the cell's response to DNA damage and developmentally induced chemotaxis (Fig. 3) (9, 24, 30).

SMEK positively regulates PP4C function during development. Our phenotypic data and the data of others (13) demonstrate that *pppC* and *smkA* have very similar effects on multicellular development, chemotaxis, and resistance to cytotoxic agents, suggesting that SMEK and PP4C function together in the same pathway for these biological processes. However, to date there is no evidence for the direct regulation of PP4C by SMEK. To examine the relationship between *smkA* and *pppC*, we performed epistasis analysis with SMEK-overexpressing and *pppC*⁻ strains. SMEK-overexpressing cells exhibit reduced aggregation, whereas *pppC*⁻ cells aggregate normally but arrest at the mound stage (30). We constructed *pppC*⁻ cells that overexpressed SMEK and examined their phenotypes. We found that *pppC*⁻ SMEK-overexpressing cells aggregated and arrested at the mound stage, just like *pppC*⁻ cells (Fig. 6A). Thus, *pppC* is epistatic to *smkA*. Since SMEK overexpression requires PP4C to cause a mutant developmental phenotype, SMEK likely functions through PP4C. As the SMEK-overexpressing cells did not phenotypically resemble *pppC*⁻ cells, these data indicate that SMEK is a positive, rather than a negative, regulator of PP4C.

Phosphatase regulatory subunits can modulate their respective catalytic subunits by modifying the catalytic activity, protein localization, and/or substrate specificity. We examined whether SMEK regulates the level of PP4C activity by immunoprecipitating the PP4C-PP4R2-SMEK complex with T7-PP4R2 and determining the associated Ser/Thr phosphatase activity. This approach allowed us to analyze PP4C activity without overexpressing the catalytic subunit of the phosphatase, which can saturate the endogenous regulatory subunits and lead to large amounts of unregulated catalytic subunit activity (21). We performed the assay with increasing protein input (cell number) and increasing duration to determine the conditions for assay linearity with protein input and with time. Importantly, PP4C activity in *smkA*⁻ cells did not

significantly differ from that in wild-type or *mek1*⁻ cells (Fig. 6B; Table 1). These findings indicate that SMEK is not an overt regulator of the PP4C-PP4R2 activity.

We previously demonstrated that SMEK translocates from the cell cortex to the nucleus upon starvation (30) and that PP4C physically interacts with the nucleus-localized SMEK^{ΔEVH1} but not with the cytoplasm-localized EVH1 (Fig. 1B). Thus, we hypothesized that SMEK regulates PP4C by controlling its subcellular localization. We examined HA-PP4C localization in cells with and without co-overexpressed V5-SMEK and found that PP4C localized to the cytoplasm in vegetative and aggregation-competent cells (Fig. 6C) and that the co-overexpression of SMEK caused PP4C to localize to the nucleus in aggregation-competent cells (Fig. 6D). We propose that SMEK may regulate PP4C translocation to the nucleus and thereby regulate PP4C substrate accessibility. The cytoplasmic localization of HA-PP4C in cells that do not overexpress SMEK but do contain endogenous SMEK is attributed to a level of SMEK protein insufficient to form a complex and regulate the elevated level of overexpressed HA-PP4C. Because of the issue of stoichiometry in dealing with biochemical complexes, especially when one member (such as PP4C) can interact in many different complexes, future studies with endogenous antibodies or knock-in mutants will be critical to understanding SMEK's regulation of PP4C.

DISCUSSION

PP4-SMEK regulates multicellular development and chemotaxis. The exact relationship between *Dictyostelium mek1* and the second-site suppressor *smkA* has been unclear due to the multifaceted development and chemotaxis phenotypes of the single and double *mek1*⁻ and *smkA*⁻ mutant strains (30). Both the yeast and mammalian SMEK homologs form complexes with the protein phosphatase 4 catalytic and regulatory subunits, PP4C and PP4R2 (8, 13, 24). We demonstrate that *Dictyostelium* SMEK also physically interacts with PP4C. Similar to SMEK, PP4C Ser/Thr phosphatase activity is required for the exit from the mound stage during multicellular development and for the manifestation of the *mek1*⁻ mutant development and chemotaxis defects. Annotation analyses of genes differentially expressed among *mek1*, *pppC*, and *smkA* mutant strains reveal that PP4C and SMEK are involved in regulating stress and cell motility genes, similar to their counterparts in yeast and mammalian systems (13, 45). During the evolution of *Dictyostelium*, PP4C's conserved role in regulating cellular responses to stress might have adapted to function in development and chemotaxis, which in *Dictyostelium* are elicited by starvation.

The similarity between the *smkA*⁻ and *pppC*⁻ development and chemotaxis phenotypes (in both the wild-type and *mek1*⁻ mutant genetic backgrounds) suggests that *smkA* and *pppC* function in the same pathway for development and chemotaxis. PP4C and the SMEK homologs PP4R3 and SMK-1 have conserved roles comparable to those of cisplatin and other cytotoxic agents in regulating cellular resistance (24, 27, 44). However, *Dictyostelium smkA*⁻ cells exhibit a less severe developmental arrest than *pppC*⁻ cells, supporting the notion that PP4C has SMEK-independent functions during development. Indeed, PP4C forms SMEK-independent complexes,

such as the PP4C-PP4R1 dimer, which inhibits histone deacetylase 3 activity, and the PP4C- α 4-CCT complex (12, 13). The loss of such SMEK-independent PP4 activity in *pppC*⁻ mutant phosphatase assays separated *pppC* and *smkA* in the dendrograms based on chemotaxis and phosphatase activity measurements, highlighting the utility of global gene expression profiles rather than individual phenotypic readouts in determining intergene relationships. In conclusion, we suggest that *smkA* regulates *pppC* to induce a subset of the functions of *pppC*, including those involving the PP4C-mediated exit from the mound stage, chemotaxis, and the expression of genes involved in cellular responses to stress and cell movement.

A *mek-pppC-smkA* genetic pathway. Our initial studies revealed that the loss of either *smkA* or *pppC* suppressed the *mek1*⁻ developmental and chemotaxis phenotypes, suggesting that *mek1* inhibits *smkA* and *pppC* function during these processes. Epistasis analysis based on the statistical differences between the unbiased global gene expression phenotypes also indicated that *pppC* and *smkA* function downstream of *mek1*. Thus, the loss of *mek1* should lead to increased or aberrant *pppC-smkA* function which could be suppressed by the loss of *smkA* or *pppC*. This pattern is what we observed in our phenotypic genetic analysis. Biochemical studies with other systems indicate that SMEK is a regulatory subunit for the PP4 catalytic subunit (12, 13, 15, 24). The similarity between the *smkA* and *pppC* developmental, chemotaxis, and gene expression phenotypes suggests that SMEK regulates PP4C activity towards specific substrates relevant to these processes. We utilized classical genetic epistasis analysis to further examine whether *smkA* positively regulates *pppC* activity during development. As *pppC*⁻ SMEK-overexpressing cells phenotypically resemble *pppC*⁻ cells, we conclude that *smkA* activates *pppC*.

The regulatory subunits of other PP2A family phosphatases, such as the B subunits of PP2A, regulate the activity, localization, and/or substrate specificity of the corresponding catalytic subunit (38). We determined that SMEK is not involved in regulating the absolute level of PP4C activity. In mammals and *Drosophila*, PP4C and PP4R2 are found throughout the cytoplasm and nucleus during interphase and localize specifically to centrosomes during mitosis (7, 15, 18, 39). In *Dictyostelium*, SMEK specifically translocates from the cytoplasm to the nucleus in response to starvation (30). We suggest that SMEK may regulate the subcellular localization of PP4C in order to control PP4C function during development and chemotaxis. We show here that the overexpression of SMEK with PP4C increased the nuclear accumulation of PP4C. While PP4C coimmunoprecipitates with the constitutively nucleus-localized SMEK^{ΔEVHI} mutant, PP4C also coimmunoprecipitates with SMEK in both vegetative and chemotaxis-competent cells, independent of SMEK's subcellular localization. Thus, we hypothesize that a preexisting cytoplasmic PP4C-SMEK complex receives the starvation signal and translocates into the nucleus. By altering PP4C localization, SMEK may regulate PP4C substrate availability, interaction, or specificity. Our biochemical results are both internally consistent and consistent with the genetic results, but they must be interpreted with caution because they rely on the use of overexpressed, tagged proteins. Nevertheless, the correlation between the functions and the subcellular localizations of the complexes in evolutionarily dis-

tant organisms and in unrelated cellular processes suggests a common regulatory mechanism for this protein phosphatase.

In conclusion, a linear *mek1-pppC-smkA* genetic pathway regulates multicellular development and chemotaxis and gene expression for these processes, previously unknown functions of PP4. However, our finding that mutations in *mek1* also suppress the developmental delays of *smkA*⁻ and *pppC*⁻ cells indicates that the overall MEK1 and PP4C-SMEK genetic and biochemical interaction is more complex. In addition, PP4C-SMEK likely has cytoplasmic functions unrelated to MEK1-regulated chemotaxis, such as those involving cell growth and survival (30). Thus, we propose that the MEK-ERK/MAPK pathway and nuclear PP4C-SMEK function in independent but intersecting pathways to regulate cellular resistance to stress and the transition of single cells moving by chemotaxis into multicellular structures. More biochemical studies will be needed to determine if a feedback loop is involved. It would be interesting to know if the *mek1-pppC-smkA* role in development and chemotaxis is conserved in other biological systems, similar to the role of *pppC-smkA* in responding to stress.

ACKNOWLEDGMENTS

We thank Eric L. Snyder for his help with the PP4 Ser/Thr phosphatase assay.

M.C.M. was supported, in part, by a Public Health Service predoctoral training grant (T32 GM08666-08). This work was supported by Public Health Service grants to R.A.F. (GM062847, GM037830, and GM0247279) and a National Institute of Child Health and Human Development grant to G.S. (PO1 HD39691).

REFERENCES

- Affolter, M., and C. J. Weijer. 2005. Signaling to cytoskeletal dynamics during chemotaxis. *Dev. Cell* **9**:19–34.
- Andreeva, A. V., and M. A. Kutuzov. 2001. PPP family of protein Ser/Thr phosphatases: two distinct branches? *Mol. Biol. Evol.* **18**:448–452.
- Aubry, L., and R. Firtel. 1999. Integration of signaling networks that regulate *Dictyostelium* differentiation. *Annu. Rev. Cell Dev. Biol.* **15**:469–517.
- Barford, D. 1996. Molecular mechanisms of the protein serine/threonine phosphatases. *Trends Biochem. Sci.* **21**:407–412.
- Barford, D., A. K. Das, and M. P. Eglhoff. 1998. The structure and mechanism of protein phosphatases: insights into catalysis and regulation. *Annu. Rev. Biophys. Biomol. Struct.* **27**:133–164.
- Booth, E. O., N. Van Driessche, O. Zhuchenko, A. Kuspa, and G. Shaulsky. 2005. Microarray phenotyping in *Dictyostelium* reveals a regulon of chemotaxis genes. *Bioinformatics* **21**:4371–4377.
- Brewis, N. D., A. J. Street, A. R. Prescott, and P. T. Cohen. 1993. PPX, a novel protein serine/threonine phosphatase localized to centrosomes. *EMBO J.* **12**:987–996.
- Carnegie, G. K., J. E. Sleeman, N. Morrice, C. J. Hastie, M. W. Pegg, A. Philp, A. I. Lamond, and P. T. Cohen. 2003. Protein phosphatase 4 interacts with the Survival of Motor Neurons complex and enhances the temporal localisation of snRNPs. *J. Cell Sci.* **116**:1905–1913.
- Cohen, P. T., A. Philp, and C. Vazquez-Martin. 2005. Protein phosphatase 4: from obscurity to vital functions. *FEBS Lett.* **579**:3278–3286.
- Dormann, D., and C. J. Weijer. 2003. Chemotactic cell movement during development. *Curr. Opin. Genet. Dev.* **13**:358–364.
- Dynes, J. L., A. M. Clark, G. Shaulsky, A. Kuspa, W. F. Loomis, and R. A. Firtel. 1994. LagC is required for cell-cell interactions that are essential for cell-type differentiation in *Dictyostelium*. *Genes Dev.* **8**:948–958.
- Gavin, A. C., M. Bosche, R. Krause, P. Grandi, M. Marzioch, A. Bauer, J. Schultz, J. M. Rick, A. M. Michon, C. M. Cruciat, M. Remor, C. Hofert, M. Schelder, M. Brajenovic, H. Ruffner, A. Merino, K. Klein, M. Hudak, D. Dickson, T. Rudi, V. Gnau, A. Bauch, S. Bastuck, B. Huhse, C. Leutwein, M. A. Heurtier, R. R. Copley, A. Edelmann, E. Querfurth, V. Rybin, G. Drewes, M. Raida, T. Bouwmeester, P. Bork, B. Seraphin, B. Kuster, G. Neubauer, and G. Superti-Furga. 2002. Functional organization of the yeast proteome by systematic analysis of protein complexes. *Nature* **415**:141–147.
- Gingras, A. C., M. Caballero, M. Zarske, A. Sanchez, T. R. Hazbun, A. Fields, N. Sonenberg, E. Hafen, B. Raught, and R. Aebersold. 2005. A novel, evolutionarily conserved protein phosphatase complex involved in cisplatin sensitivity. *Mol. Cell Proteomics* **4**:1725–1740.
- Giroux, S., M. Tremblay, D. Bernard, J.-F. Cadrin-Girard, S. Aubry, L.

- Larouche, S. Rousseau, J. Huot, L. Jeannotte, and J. Charron. 1999. Embryonic death of Mek1-deficient mice reveals a role for this kinase in angiogenesis in the labyrinthine region of the placenta. *Curr. Biol.* **9**:369–372.
15. Hastie, C. J., G. K. Carnegie, N. Morrice, and P. T. Cohen. 2000. A novel 50 kDa protein forms complexes with protein phosphatase 4 and is located at centrosomal microtubule organizing centres. *Biochem. J.* **347**:845–855.
 16. Hastie, C. J., and P. T. Cohen. 1998. Purification of protein phosphatase 4 catalytic subunit: inhibition by the antitumour drug fostriecin and other tumour suppressors and promoters. *FEBS Lett.* **431**:357–361.
 17. Hazzalin, C. A., and L. C. Mahadevan. 2002. MAPK-regulated transcription: a continuously variable gene switch. *Nat. Rev. Mol. Cell Biol.* **3**:30–40.
 18. Helps, N. R., N. D. Brewis, K. Linneruth, T. Davis, K. Kaiser, and P. T. Cohen. 1998. Protein phosphatase 4 is an essential enzyme required for organisation of microtubules at centrosomes in *Drosophila* embryos. *J. Cell Sci.* **111**:1331–1340.
 19. Howard, P. K., K. G. Ahern, and R. A. Firtel. 1988. Establishment of a transient expression system for Dictyostelium discoideum. *Nucleic Acids Res.* **16**:2613–2623.
 20. Insall, R. H., R. D. Soede, P. Schaap, and P. N. Devreotes. 1994. Two cAMP receptors activate common signaling pathways in Dictyostelium. *Mol. Biol. Cell* **5**:703–711.
 21. Janssens, V., and J. Goris. 2001. Protein phosphatase 2A: a highly regulated family of serine/threonine phosphatases implicated in cell growth and signalling. *Biochem. J.* **353**:417–439.
 22. Juvan, P., J. Demsar, G. Shaulsky, and B. Zupan. 2005. GenePath: from mutations to genetic networks and back. *Nucleic Acids Res.* **33**:W749–W752.
 23. Katoh, M., C. Shaw, Q. Xu, N. Van Driessche, T. Morio, H. Kuwayama, S. Obara, H. Urushihara, Y. Tanaka, and G. Shaulsky. 2004. An orderly retreat: dedifferentiation is a regulated process. *Proc. Natl. Acad. Sci. USA* **101**:7005–7010.
 24. Keogh, M. C., J. A. Kim, M. Downey, J. Fillingham, D. Chowdhury, J. C. Harrison, M. Onishi, N. Datta, S. Galicia, A. Emili, J. Lieberman, X. Shen, S. Buratowski, J. E. Haber, D. Durocher, J. F. Greenblatt, and N. J. Krogan. 2006. A phosphatase complex that dephosphorylates gammaH2AX regulates DNA damage checkpoint recovery. *Nature* **439**:497–501.
 25. Kimmel, A. R., and R. A. Firtel. 2004. Breaking symmetries: regulation of Dictyostelium development through chemoattractant and morphogen signal-response. *Curr. Opin. Genet. Dev.* **14**:540–549.
 26. Kloeker, S., and B. E. Wadzinski. 1999. Purification and identification of a novel subunit of protein serine/threonine phosphatase 4. *J. Biol. Chem.* **274**:5339–5347.
 27. Ma, H., M. Gamper, C. Parent, and R. A. Firtel. 1997. The Dictyostelium MAP kinase kinase DdMEK1 regulates chemotaxis and is essential for chemoattractant-mediated activation of guanylyl cyclase. *EMBO J.* **16**:4317–4332.
 28. Manahan, C. L., P. A. Iglesias, Y. Long, and P. N. Devreotes. 2004. Chemoattractant signaling in Dictyostelium discoideum. *Annu. Rev. Cell Dev. Biol.* **20**:223–253.
 29. Mendoza, M., and R. A. Firtel. 2006. Assaying chemotaxis of Dictyostelium cells, p. 393–406. *In* L. Eichinger and F. Rivero-Crespo (ed.), *Dictyostelium discoideum Protocols*. Humana Press, Totowa, NJ.
 30. Mendoza, M. C., F. Du, N. Iranfar, N. Tang, H. Ma, W. F. Loomis, and R. A. Firtel. 2005. Loss of SMEK, a novel, conserved protein, suppresses MEK1 null cell polarity, chemotaxis, and gene expression defects. *Mol. Cell. Biol.* **25**:7839–7853.
 31. Murphy, L. O., and J. Blenis. 2006. MAPK signal specificity: the right place at the right time. *Trends Biomed. Sci.* **31**:268–274.
 32. Myles, T., K. Schmidt, D. R. Evans, P. Cron, and B. A. Hemmings. 2001. Active-site mutations impairing the catalytic function of the catalytic subunit of human protein phosphatase 2A permit baculovirus-mediated overexpression in insect cells. *Biochem. J.* **357**:225–232.
 33. O'Brien, L. E., K. Tang, E. S. Kats, A. Schultz-Geshwender, J. H. Lipschutz, and K. E. Mostov. 2004. ERKs and MMPs sequentially regulate distinct stages of epithelial tubule development. *Dev. Cell* **7**:21–32.
 34. Parent, C. A. 2004. Making all the right moves: chemotaxis in neutrophils and Dictyostelium. *Curr. Opin. Cell Biol.* **16**:4–13.
 35. Pritchard, C. A., L. Hayes, L. Wojnowski, A. Zimmer, R. M. Marais, and J. C. Norman. 2004. B-Raf acts via the ROCKII/LIMK/Cofilin pathway to maintain actin stress fibers in fibroblasts. *Mol. Cell. Biol.* **24**:5937–5952.
 36. Roux, P. P., and J. Blenis. 2004. ERK and p38 MAPK-activated protein kinases: a family of protein kinases with diverse biological functions. *Microbiol. Mol. Biol. Rev.* **68**:320–344.
 37. Sobko, A., H. Ma, and R. A. Firtel. 2002. Regulated SUMOylation and ubiquitination of DdMEK1 is required for proper chemotaxis. *Dev. Cell* **2**:745–756.
 38. Sontag, E. 2001. Protein phosphatase 2A: the Trojan horse of cellular signaling. *Cell. Signal.* **13**:7–16.
 39. Sumiyoshi, E., A. Sugimoto, and M. Yamamoto. 2002. Protein phosphatase 4 is required for centrosome maturation in mitosis and sperm meiosis in *C. elegans*. *J. Cell Sci.* **115**:1403–1410.
 40. Sutoh, K. 1993. A transformation vector for Dictyostelium discoideum with a new selectable marker bsr. *Plasmid* **30**:150–154.
 41. Van Driessche, N., J. Demsar, E. O. Booth, P. Hill, P. Juvan, B. Zupan, A. Kuspa, and G. Shaulsky. 2005. Epistasis analysis with global transcriptional phenotypes. *Nat. Genet.* **37**:471–477.
 42. Van Driessche, N., C. Shaw, M. Katoh, T. Morio, R. Sugang, M. Ibarra, H. Kuwayama, T. Saito, H. Urushihara, M. Maeda, I. Takeuchi, H. Ochiai, W. Eaton, J. Tollett, J. Halter, A. Kuspa, Y. Tanaka, and G. Shaulsky. 2002. A transcriptional profile of multicellular development in Dictyostelium discoideum. *Development* **129**:1543–1552.
 43. Wessels, D., and D. R. Soll. 1998. Computer-assisted characterization of the behavioral defects of cytoskeletal mutants of *Dictyostelium discoideum*, p. 101–140. *In* D. R. Soll and D. Wessels (ed.), *Motion analysis of living cells*. Wiley-Liss, New York, NY.
 44. Wolff, S., H. Ma, D. Burch, G. A. Maciel, T. Hunter, and A. Dillin. 2006. SMK-1, an essential regulator of DAF-16-mediated longevity. *Cell* **124**:1039–1053.
 45. Wu, H. L., J. A. Brown, M. J. Dorie, L. Lazzeroni, and J. M. Brown. 2004. Genome-wide identification of genes conferring resistance to the anticancer agents cisplatin, oxaliplatin, and mitomycin C. *Cancer Res.* **64**:3940–3948.
 46. Xu, Q., M. Ibarra, D. Mahadeo, C. Shaw, E. Huang, A. Kuspa, D. Cotter, and G. Shaulsky. 2004. Transcriptional transitions during *Dictyostelium* spore germination. *Eukaryot. Cell* **3**:1101–1110.
 47. Xu, Q., and G. Shaulsky. 2005. GOAT: an R tool for analysing gene ontology trade mark term enrichment. *Appl. Bioinformatics.* **4**:281–283.
 48. Yujiri, T., S. Sather, G. R. Fanger, and G. L. Johnson. 1998. Role of MEKK1 in cell survival and activation of JNK and ERK pathways defined by targeted gene disruption. *Science* **282**:1911–1914.
 49. Zhang, X., Y. Ozawa, H. Lee, Y.-D. Wen, T.-H. Tan, B. E. Wadzinski, and E. Seto. 2005. Histone deacetylase 3 (HDAC3) activity is regulated by interaction with protein serine/threonine phosphatase 4. *Genes Dev.* **19**:827–839.
 50. Zupan, B., J. Demsar, I. Bratko, P. Juvan, J. A. Halter, A. Kuspa, and G. Shaulsky. 2003. GenePath: a system for automated construction of genetic networks from mutant data. *Bioinformatics* **19**:383–389.